Tensile Properties of *Argiope trifasciata* Drag Line Silk Obtained from the Spider's Web

J. PÉREZ-RIGUEIRO,[1] M. ELICES,[1] J. LLORCA,[1] C. VINEY[2]

[1] Departamento de Ciencia de Materiales, Universidad Politécnica de Madrid, ETS de Ingenieros de Caminos, Ciudad Universitaria, 28040 Madrid, Spain

[2] Department of Chemistry, Heriot-Watt University, Edinburgh EH14 4AS, Scotland

Received 2 August 2000; accepted 20 January 2001

ABSTRACT: The tensile properties of *Argiope trifasciata* (Argiopidae) drag line silk retrieved from mooring threads in the web were characterized. Scanning electron microscope images were used to determine the cross-sectional area of the samples, allowing force-displacement plots to be rescaled as stress–strain curves and to characterize fracture surfaces. Twenty-eight samples were tested to obtain statistically significant values of the mechanical parameters (elastic modulus, stress and strain at the proportional limit, and tensile strength). The tensile strength of the material was subjected to a Weibull analysis—the first time that this has been attempted with a spider silk. A low value of the Weibull modulus, $m = 3.4$, was obtained, demonstrating that drag line monofilament does not have a sufficiently reliable tensile strength to function as an engineering material on its own. © 2001 John Wiley & Sons, Inc. J Appl Polym Sci 82: 2245–2251, 2001

Key words: spider silk; fibers; fracture; mechanical properties; Weibull modulus

INTRODUCTION

It has long been recognized that spider silks exhibit unique combinations of strength, stiffness, and toughness which are unrivaled by either man-made or other natural fibers.[1,2] This view is supported by a diffuse literature of experimental data generated over the last 40 years.[3–12] The measured strength values reported in previous articles suggest a wide experimental scatter, which can be attributed, in part, to the intrinsic variability of biological materials. However, this variability is exacerbated in the case of silk by the experimental difficulties of characterizing the irregular and small (2–5-μm diameter) sample cross sections accurately. Early studies[5–7] relied on light microscopy to determine the fiber diameter, but the intrinsic limitation of this technique led to uncertainties of up to 60% in the actual values of the fiber cross-sectional area.[5,6] Moreover, the variability in the cross-sectional area along the length of the fiber was not considered.

More recent investigations used a scanning electron microscope[8,9,11–13] or laser diffraction[10] to measure the diameter along the fiber and computed an average value from which to determine the area. These approaches provided accurate data on the strength and stiffness of various spider silks, revealing large differences in the tensile properties of silk from different spiders. Large variations were also found among silks obtained from different individuals of the same species and from the same individual.[14] The highest average

Correspondence to: J. Pérez-Rigueiro.

Contract grant sponsors: Ministerio de Educación y Cultura (Spain); British Council.

Journal of Applied Polymer Science, Vol. 82, 2245–2251 (2001)

strength (1.7 GPa) was measured for *Nephila clavipes* major ampullate silk,[10] whereas the lowest (around 0.8 GPa) was obtained from *Araneus diadematus* major ampullate silk.[13] All these studies were limited by the tedious procedure of characterizing the sample diameter. The number of samples analyzed was therefore small (in the range of 1–6 for each silk studied),[8–13] restricting the statistical significance of these data.

It is not surprising that silk from different spider species exhibit diverse mechanical properties, since the material must behave reliably under a range of in-service conditions. To develop our overall understanding of silk behavior, it is necessary to characterize the mechanical properties in a way that reveals clearly the differences and similarities among various silks. To distinguish interspecies differences from the intrinsic variability of this material, an appropriately large number of tests must be performed under carefully controlled conditions on silk samples that have been collected so as to minimize scatter. It is also necessary to use appropriate statistical tools when interpreting the results (especially the strength values, which tend to be more variable than the other tensile parameters). Among the different types of spider silk, drag line achieves the highest tensile strength and has been the most widely studied. Our present work focused on the tensile properties of drag line silk collected directly from the web of *Argiope trifasciata* (Argiopidae). The tensile behavior of 28 fibers was characterized. Force-displacement data from the tests were rescaled as stress–strain curves, using the fiber cross section as determined by scanning electron microscopy (SEM). This information was sufficient to obtain statistically significant data on the fiber properties and, in particular, to compute the Weibull parameters for the fiber breaking strength.

EXPERIMENTAL

An *A. trifasciata* spider was kept in a box 70 × 70 × 20 cm and fed a diet of crickets. A wooden frame was placed in the box, so that the spider could build webs. All the silk used in this study was collected from a single web to reduce the possible sources of variability. Drag line silk is used to produce the mooring threads, framework threads, and radials in the web (Fig. 1).[15,16] The mounting and tensile test procedures were described and illustrated in detail elsewhere.[17,18] Samples from

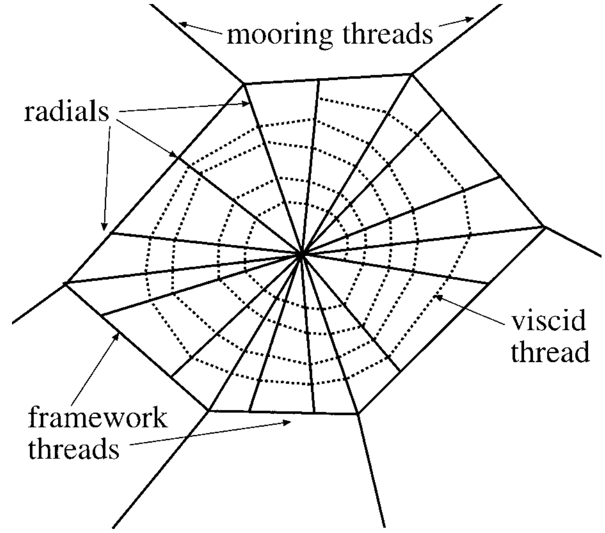

Figure 1 Macrostructure of a spider web. Solid lines denote the components that are made from drag line.

these web components were cut and, when possible, separated carefully into individual monofilaments. These were then glued across holes cut in pieces of cardboard, defining a gauge length of 20 mm.

Tensile tests were performed with an Instron 4411 machine at a constant crosshead speed to achieve an average strain rate of 2×10^{-4} s^{-1}. The load applied to the sample was measured with a balance (Precisa 6100 C, resolution ±10 mg) attached to the lower end of the sample.[17,18] The crosshead displacement was taken as a direct measurement of the sample deformation, since the compliance of silk is approximately 1000 times larger than that of the equipment.[17] The tests were performed in air under nominal conditions of 20°C and 60% relative humidity.

After testing, some of the samples were retrieved and sputtered with gold. They were examined in a JEOL 6300 scanning electron microscope (observation conditions $V = 10$ kV, $I = 0.06$ nA). The images were used to confirm the presence of a single filament in each sample and to measure the sample diameter at different positions along the gauge length. The fracture surfaces of the samples were also studied.

RESULTS AND DISCUSSION

Selection of Material for Testing

The harvesting of naturally spun material from webs was preferred to forced silking so that the

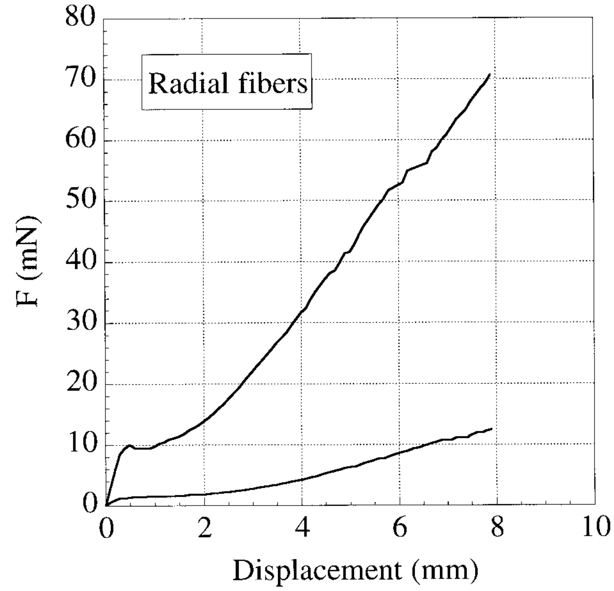

Figure 2 Force-displacement curves of two radials from an *A. trifasciata* web, illustrating the significant variability of this material.

results of this work might reflect the properties of natural material as closely as possible. Therefore, the initial task was to select the material to be tested from among the different elements of the web: mooring threads, framework threads, and radials (see Fig. 1). Preliminary tests revealed significant variability in the behavior of radials, as illustrated in Figure 2. These differences arise because the spider introduces new filaments alongside the existing ones as it rebuilds the web,[19] so the number of filaments in any radial is not constant along its length. It would be helpful if individual monofilaments could be tested; however, the presence of viscid thread residue impedes the separation of the radials into their constituent monofilaments. Similarly, it was not possible to isolate monofilaments from framework threads, due to the adhesive protein that is present at the points where the framework and radial threads intersect. In contrast, mooring threads are easy to collect and divide into individual monofilaments, so we conducted our study on this material.

The force-displacement curves of three adjacent samples cut from a monofilament were compared (Fig. 3) to check whether the mechanical properties vary along the monofilament. The force-displacement curves of such adjacent samples follow closely similar paths, but the loads and extensions which they can sustain before breaking are highly variable. Similar tensile deformation characteristics of adjacent samples cut from a thread was recognized previously for silkworm cocoon silk[17] and for drag line obtained by forced silking of spiders.[20]

The possibility of altering the properties of silk during manipulation must be considered, since monofilaments are extremely delicate and prone to stretching while being handled. We are careful to minimize the loading on samples as they are prepared for testing. Also, the existence of a true elastic region and recognizable yield point in the mechanical response (Fig. 3) means that small deformations can be tolerated without a permanent effect on the tensile properties.[17]

Sample Geometry

After tensile testing, the geometry of 13 samples, each from a different monofilament, was studied by SEM. To representatively characterize the variability of this material, we specifically chose *non*adjacent samples for this study. To allow for variations in the cross-sectional area and shape, micrographs were recorded at two different positions along the sample, in each case at two different orientations (0°–50°).[17,18] The orientation was changed by rotating the sample about its long

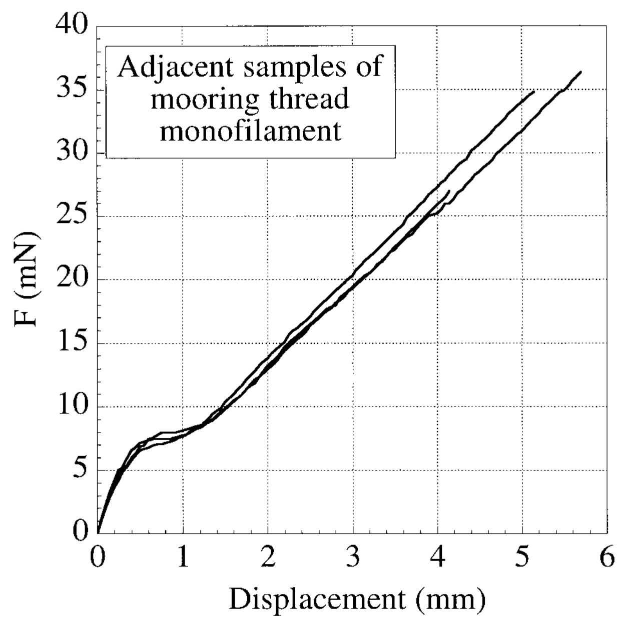

Figure 3 Force-displacement curves of three samples cut successively from a single monofilament of mooring thread. The curves superimpose closely, but the loads and extensions sustained by the samples before breaking are highly variable.

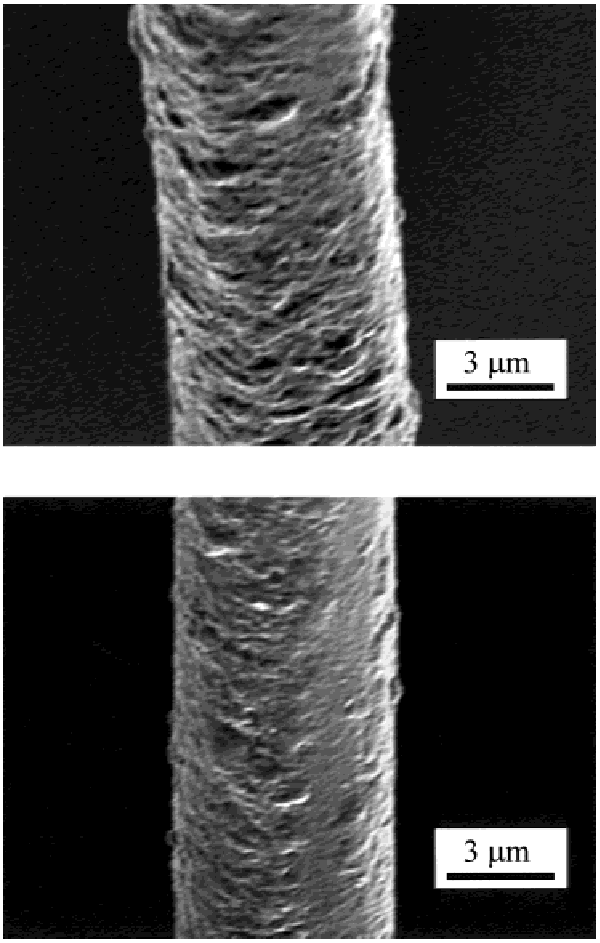

Figure 4 Scanning electron microscopy images of *A. trifasciata* drag line monofilament. The two orientations are related by a 50° rotation about the long axis of the sample.

axis in the microscope. Ideally, the two orientations would have differed by 90°, but we were limited by the geometrical specifications of the microscope. An example of a pair of micrographs recorded at 0° and 50° is shown in Figure 4.

Results are summarized in Table I, where the average monofilament diameter, D, maximum diameter, D_{max}, minimum diameter, D_{min}, and average shape anisotropy are presented. The shape anisotropy is calculated as the ratio of D_0 (or D_{50}, whichever number is greater) to D_{50} (or D_0, whichever number is smaller); subscripts denote the sample orientation. For each monofilament, the four measurements of the diameter differed by less than 5%. This relative uniformity of the cross-sectional geometry contrasts with the highly variable cross section of the drag line obtained by forced silking of spiders.[7,10] If the comparison is made with silkworm (*Bombyx mori*) monofilament silk (brin),[18] we find that *A. trifasciata* drag line exhibits a similar variability of D along the monofilaments and its cross section approaches a circular geometry more closely (shape anisotropy = 1.05 for *A. trifasciata* drag line and 1.16 for silkworm silk). The circular cross-section of *A. trifasciata* drag line is also observed in fracture surfaces (see below), in comparison with the more ellipsoidal cross section of *B. mori* fracture surfaces.[17]

Stress–Strain Response

The average diameter of each sample characterized by SEM was used to calculate its area, assuming a circular cross section. Since the samples were observed in the microscope *after* tensile testing, we assumed that the measured area of the fractured sample was related to the initial area through the equation

$$A_f = A_0 l_0 / l_f \tag{1}$$

Equation (1) implies that the volume of the sample remains constant during the tensile test and is used consistently with previous work on silkworm silk.[17,18] The initial cross-sectional area is needed to obtain stress–strain curves from the force-displacement data.

Because we demonstrated that (a) adjacent samples cut from a given monofilament exhibit very similar behavior in tensile tests (Fig. 3) and (b) cross-sectional geometry does not vary significantly along each monofilament, we are able to use the measured sample areas to also characterize the cross-sectional area of adjacent samples cut from the same monofilament. In this way, we obtained stress–strain curves from a total of 28 samples.

Some representative stress–strain curves are shown in Figure 5. It is apparent that the *A. trifasciata* web drag line is highly variable when samples from different monofilaments are consid-

Table I Geometrical Parameters of *A. trifasciata* Drag Line Monofilament Harvested from the Web

D (μm)	D_{max} (μm)	D_{min} (μm)	Shape Anisotropy
6.6 ± 0.2	8.5	5.0	1.05 ± 0.01

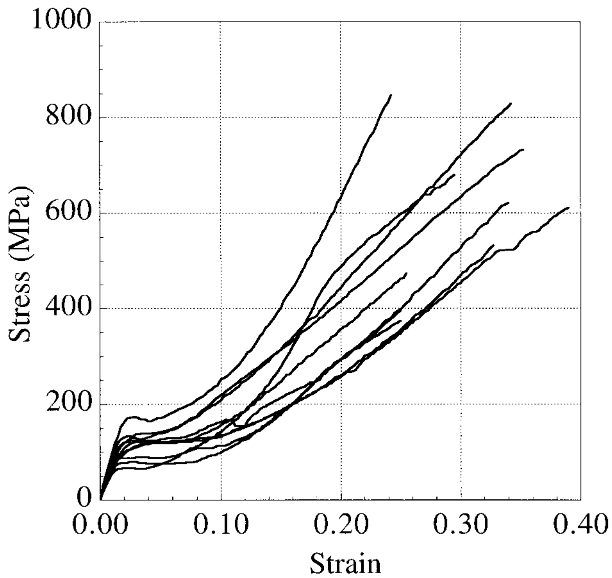

Figure 5 Representative stress–strain curves of *A. trifasciata* drag line silk harvested from the web, showing the behavior of samples obtained from several monofilaments.

ered. Tensile parameters collated from the stress–strain curves are presented in Table II, alongside the corresponding values for *B. mori* silkworm silk. Stress and strain at the proportional limit are denoted by σ_p and ε_p, respectively. (The proportional limit is defined as the point where a force-displacement curve intersects a straight line which passes through the origin and has a slope equal to 95% of the initial slope of the curve.[21]) The energy required to deform a unit volume of the material to failure can be calculated from the area under the stress–strain curve and is denoted by W_f.

If the properties of *A. trifasciata* drag line are compared with those of silkworm silk, it is evident that the drag line has a lower elastic modulus and a lower stress at the proportional limit. The strain at the proportional limit is very similar in both silks. Both materials exhibit similar average values of tensile strength, but the drag line sustains a significantly greater elongation to break. The value of W_f obtained for the drag line is almost double the value found for silkworm silk (computed from the stress–strain curves presented in ref. 18). Overall, therefore, the drag line is more able to accommodate large deflections. This finding is not unexpected when the materials are considered in their natural context, since the biological functions of drag line and silkworm silk are very different. Even though most of the energy transferred from a captured prey is dissipated by the viscid thread in the web, the drag line must also be able to absorb energy if stretched past its proportional limit—otherwise, the integrity of the web would be easily destroyed. Silkworm silk, on the other hand, is used in the form of a dense composite mat which acts as a shelter for the pupa. It is important that this structure should resist large deflections, so that the contents are not easily bruised or crushed.

Fracture Surface Characterization

Figure 6 shows a scanning electron micrograph of a typical fracture surface. The surface is transverse to the fiber and exhibits roughness on a scale of approximately 1 μm. No significant change in the sample diameter was observed when the fracture surfaces were compared with other regions of the sample, which suggests that deformation occurred uniformly along the fiber rather than being localized in a neck. The features of the fracture surface are similar to those reported by Cunniff et al.[9] for drag line silk obtained from *Nephila clavipes* spiders by forced silking and tested at 10 %/s. Work[7] also presented a similarly rough fracture surface for *Nephila clavipes* drag line (again obtained by forced silking, but tested at a rate of 1.6 %/s). However, he indicated (without elaboration) that different features were observed in silk harvested directly from the web. Because we observed fracture surfaces after testing the silk at a significantly lower

Table II Tensile Properties of *A. trifasciata* Drag Line Silk Harvested from the Web

	E (GPa)	σ_p (MPa)	ε_p	σ_u (MPa)	ε_u	W_f (MJ/m^3)
A. trifasciata	6.9 ± 0.4	80 ± 10	0.013 ± 0.001	600 ± 50	0.30 ± 0.02	90 ± 10
B. mori	16 ± 1	230 ± 10	0.011 ± 0.001	650 ± 40	0.12 ± 0.01	50 ± 10

Corresponding properties of *B. mori* silkworm silk[18] are shown for comparison. E, elastic modulus; σ_p, stress at proportional limit; ε_p, strain at proportional limit; σ_u, tensile strength; ε_u, strain at breaking; W_f, energy to break unit volume of material. The proportional limit is defined in the text.

strain rate than either of these previous studies (albeit using drag line from a different spider genus), we can be confident that there was more opportunity for viscous flow to occur in our samples. Conservation of volume dictates that inherently weak regions in the microstructure will more readily open into detectable voids if viscous flow can occur to a greater extent. We therefore suggest that the "mosaic" appearance of the fracture surfaces may point to a microfibrillar structure for this material, which would be consistent with the fibrillar nature of many other types of silk.[22] However, we must also recognize the possibility that this structure is an artifact—in the present case due to shrinkage as the sample dries out in the low-pressure environment required for sputter-coating and SEM imaging, and in previous research due to degumming, swelling, infiltration, or desiccation treatments involved in the specimen preparation process.

A significant opportunity for viscous flow is also likely to accentuate any skin–core microstructural differences in the sample. The fracture surfaces of our *A. trifasciata* monofilament, as exemplified in Figure 6, do show clear evidence of a skin–core microstructure, supporting other observations of such segregation in selected drag line[23,24] and silkworm silks.[25] However, this does not resolve the issue of whether the skin–core microstructure is chemical (due to compositional segregation) or physical (due to expected differences in molecular alignment of silk nearer the edge and nearer the middle of the flow cross section). The fact that fracture does not appear to nucleate at the skin–core interface suggests that there is no abrupt discontinuity here and points to a process-based origin of the microstructural gradient.

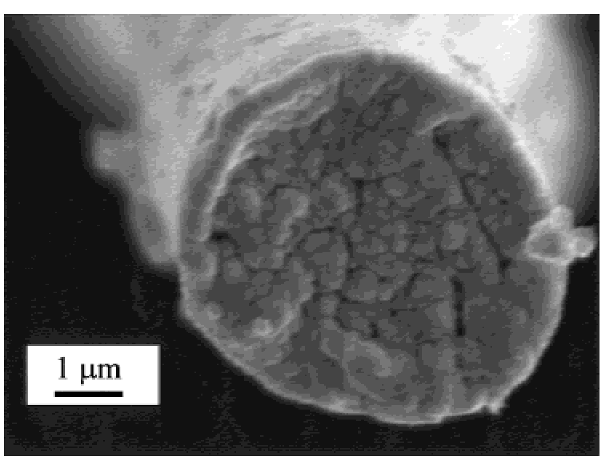

Figure 6 Scanning electron micrograph of a typical fracture surface. Imaging conditions were the same as those for sample diameter characterization.

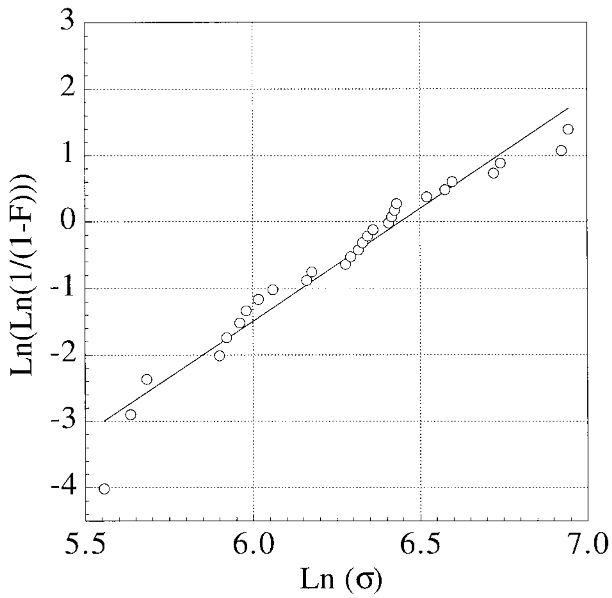

Figure 7 Weibull plot constructed from tensile-strength measurements performed on 28 samples of *A. trifasciata* drag line monofilament.

Weibull Modulus

Stress–strain data of 28 samples were used to explore the Weibull statistics of the *A. trifasciata* drag line. The computational details can be found elsewhere,[26] but the analysis is based on the construction of an Ln[Ln(1/1 − F)] versus Ln σ_u plot, where F is a measure of the probability of fracture of a sample and σ_u is its tensile strength.

If the samples follow Weibull statistics, the result of this plot is a straight line. The slope, m, is an indicator of the reproducibility of the tensile strength of the material and is known as the Weibull modulus. A high value (e.g., $m = 200$–300, as typically exhibited by ductile metals) characterizes a highly reproducible strength and provides reassurance that a material will behave reliably in an engineering context. A low value (e.g., $m = 5$, glass, or $m = 5$–25, common ceramics) characterizes materials with a poorly reproducible tensile strength. The point where an extrapolated Weibull plot intersects the y-axis, $-m$ Ln σ_0, is a measurement of the average tensile strength of the samples.

The Weibull plot constructed from our data is presented in Figure 7 and yields values of $m = 3.4$

$\pm$ 0.1 and $\sigma_0 = 609 \pm 1$ MPa. It may seem surprising that a web can rely on a low Weibull modulus material when it performs such a critical function. However, we have already noted that the web is not constructed from monofilament silk. Also, a spider web is a labile structure which must be functional for only a few days. It therefore is likely that the failure statistics of silk reflect a compromise that takes into account the required functionality and durability of the web and the metabolic cost of silk synthesis and spinning.

CONCLUSIONS

The tensile properties of drag line silk of *A. trifasciata* obtained directly from the web were determined. From the several elements of the web, the mooring threads are especially well suited for this study, because it is relatively easy to separate them into their constituent monofilaments. Adjacent samples (successive samples cut from the same monofilament) show similar tensile properties, consistently with previous data for spider silk obtained by forced silking. Scanning electron microscopy reveals that the cross-sectional geometry of the drag line monofilament retrieved from the web is significantly more uniform than that of forced silk. The cross section is approximately circular.

In comparison to *B. mori* (silkworm) silk, the drag line monofilament has a lower elastic modulus, a lower stress at the proportional limit, a similar strain at the proportional limit, a similar tensile strength, and a twofold greater energy requirement to deform a unit volume of material to the point of fracture. Fracture surfaces suggest that the material has a skin–core microstructure and that the core may consist of microfibrils. The tensile strength follows a Weibull distribution; the low value of the Weibull modulus, $m = 3.4$, implies that drag line monofilament does not have a sufficiently reliable tensile strength to be used as an engineering material on its own.

The authors would like to thank Oscar Campos and Pablo García (Naturaleza Misteriosa, Parque Zoológico de Madrid, Spain) for breeding the spider used in this work. Partial support for this work was received from the Ministerio de Educación y Cultura (Spain) and the British Council through an Acción Integrada.

REFERENCES

1. Silk Polymers. Materials Science and Biotechnology; Kaplan, D.; Adams, W. W.; Farmer, B.; Viney, C., Eds.; ACS Symposium Series 544; American Chemical Society: Washington, DC, 1994.
2. Int J Biol Macromol 1999, vol 24, parts 2 and 3, special issue on silks.
3. Lucas, F.; Shaw, J. T. B.; Smith, S. G. J Text Inst 1955, 46, 440–452.
4. Lucas, F. Discovery 1964, 25, 20–26.
5. Zemlin, J. C. Technical Report No. 69-29-CM (AD 684333); U.S. Army Natick Laboratories: Natick, MA, Sept 1968.
6. Denny, M. J Exp. Biol 1976, 65, 483–506.
7. Work, R. W. Text Res J 1976, July, 485–492.
8. Griffiths, J. R.; Salanitri, V. R. J Mater Sci 1980, 15, 491–496.
9. Cunniff, P. M.; Fossey, S. A.; Auerbach, M. A.; Song, J. W. In Silk Polymers. Materials Science and Biotechnology; Kaplan, D.; Adams, W. W.; Farmer, B.; Viney, C., Eds.; ACS Symposium Series 544; American Chemical Society: Washington, DC, 1994; pp 234–251.
10. Dunaway, D. L.; Thiel, B. L.; Viney, C. J Appl Polym Sci 1995, 58, 675–683.
11. Köhler, T.; Vollrath, F. J Exp Zool 1995, 271, 1–17.
12. Vollrath, F.; Köhler, T. Proc R Soc Lond B 1996, 263, 387–391.
13. Shao, Z.; Vollrath, F. Polymer 1999, 40, 1799–1806.
14. Madsen, B.; Shao, Z. Z.; Vollrath, F. Int J Biol Macromol 1999, 24, 301–306.
15. Kaplan, D. L.; Lombardi, S. J.; Muller, W. S.; Fossey, S. A. In Biomaterials; Byrom, D., Ed.; Stockton: New York, 1991; pp 1–53.
16. Jackson, R. R. Bull Brit Arach Soc 1973, 2, 125–126.
17. Pérez-Rigueiro, J.; Viney, C.; LLorca, J.; Elices, M. J Appl Polym Sci 1998, 70, 2439–2447.
18. Pérez-Rigueiro, J.; Viney, C.; LLorca, J.; Elices, M. J Appl Polym Sci 2000, 75, 1270–1277.
19. Vollrath, F. Int J Biol Macromol 1999, 24, 81–88.
20. Work, R. W. Text Res J 1977, 47, 650–662.
21. American Society for Testing and Materials; Standard Test Method for Plane-Strain Fracture Toughness of Metallic Materials, E-399, 1983.
22. Putthanarat, S.; Stribeck, N.; Fossey, S. A.; Eby, R. K.; Adams, W. W. Polymer 2000, 41, 7735–7747.
23. Vollrath, F.; Holtet, T.; Thøgersen, H. C.; Frische, S. Proc R Soc Lond B 1996, 263, 147–151.
24. Frische, S.; Maunsbach, A. B.; Vollrath, F. J Microsc 1998, 189, 64–70.
25. Robson, R. M. Int J Biol Macromol 1999, 24, 145–150.
26. Chou, T.-W. Microstructural Design of Fiber Composites; Cambridge University: Cambridge, 1992; pp 98–168.